Physica Scripta. Vol. 52, 516–521, 1995

Extended Analysis of Intensity Anomalies in the Al I Isoelectronic Sequence

L. Engström, M. Kirm, P. Bengtsson, S. T. Maniak[1], L. J. Curtis[1], E. Träbert[2], J. Doerfert[2] and J. Granzow[2]

Department of Physics, University of Lund, Sölvegatan 14, S-223 62 Lund, Sweden
[1] Department of Physics and Astronomy, University of Toledo, Toledo, Ohio 43606, U.S.A.
[2] Experimentalphysik III, Ruhr-Universität Bochum, D-44780 Bochum, Germany

Received March 2, 1995; accepted in revised form May 5, 1995

Abstract

This paper reports an extended experimental investigation, using the beam-foil technique, of the intensity ratio of the fine-structure components in the $3s^23p\,^2P_{1/2,\,3/2}$–$3s3p^2\,^2S_{1/2}$ and $^2P_{1/2}$ resonance transitions along the Al I isoelectronic sequence. These intensity ratios are strongly influenced by cancellation/enhancement effects arising from spin-orbit induced level mixings, and are thus sensitive probes of the detailed atomic structure. New data are given for Si II, P III, S IV, K VII, Sc IX, Fe XIV and Ni XVI. Together with previous experimental results this comprehensive isoelectronic study reveals significant and systematic deviations from theoretical predictions.

1. Introduction

The $3s^23p\,^2P_{1/2,\,3/2}$–$3s3p^2\,^2S_{1/2}$ and $^2P_{1/2}$ resonance transitions in the Al I isoelectronic sequence provide an interesting example of how interference effects may redistribute the oscillator strength among various channels. The first investigation of this problem was reported in [1], where the beam-foil technique was used to study the relative intensities of the transitions from both $3s3p^2\,^2S_{1/2}$ and $^2P_{1/2}$ to the two fine-structure levels of the ^2P ground state in S IV, Cl V, Ar VI and Ti X. The experimental intensity ratios, particularly from the $^2S_{1/2}$ level, were found to deviate significantly from the *LS* value. A similar investigation of the homologous states $2s2p^2\,^2S_{1/2}$ and $^2P_{1/2}$ in the B I sequence has also been reported [2].

A theoretical analysis in the Al-sequence showed that a qualitative explanation of the observed ratios could be obtained in a single-configuration model, by considering only the interaction between the $3s3p^2\,^2S_{1/2}$, $^2P_{1/2}$ and $^4P_{1/2}$ states [1]. Due to the different phases of the mixing coefficients this interaction leads to an enhancement in the $^2P_{1/2}$–$^2S_{1/2}$ and $^2P_{3/2}$–$^2P_{1/2}$ line strength and to a cancellation in the $^2P_{3/2}$–$^2S_{1/2}$ and $^2P_{1/2}$–$^2P_{1/2}$ channels. Hence the ratios $I(3/2\text{–}1/2)/I(1/2\text{–}1/2)$ are strongly affected. More detailed calculations, including configuration interactions within the whole $n = 3$ complex, changed the predicted intensity ratios only slightly but resulted in good agreement with the relativistic results of Huang [3] and Farrag *et al.* [4]. Compared to the experimental results good agreement was obtained for the ratios from $^2P_{1/2}$, where the predicted deviations from the *LS* value in the beginning of the sequence are rather small. However, for the transitions from $^2S_{1/2}$, where the effect is much larger, significant discrepancies were found in S IV, Cl V and Ar VI. The high-*Z* trend, on the other hand, seemed to be confirmed by the experimental value for Ti X.

In a very recent study, Kastner [5] derived the intensity ratios for the transitions from both $3s3p^2\,^2S_{1/2}$ and $^2P_{1/2}$ in Si II from solar observations [6] by taking the optical thickness of the solar source into account. The value obtained for the ^2P–^2S transitions is in perfect agreement with the theoretical results. Thus, it seemed that the discrepancy between theory and experiments, if real, is restricted to a narrow range of ions. This interesting problem stimulated the present extension of the laboratory measurements to Si II, P III, K VII, Sc IX, Fe XIV and Ni XVI, in an effort to provide a more comprehensive isoelectronic comparison between theory and experiment. The analysis of Kastner [5] shows, of course, also that once the fundamental atomic physics problem has been settled, important information about the solar opacity could be obtained using these intensity ratios.

2. Experiments

2.1. *General considerations*

The beam-foil technique is, in all respects but one, eminently suited for the measurements of relative intensities [1, 2]. First of all, the low particle density of the beam ($<10^5$ particles/cm^3) and the high vacuum environment ($<10^{-6}$ torr) eliminates the potential problems of radiation trapping or collisional deexcitation. Secondly, the photon-counting detection technique used ensures a linear intensity scale over a large dynamic range. Finally, in the present case the measurements involve closely spaced lines (typically less than 10 Å apart, see Table I) from a common upper level. Hence, no corrections for the wavelength dependent detection efficiency is really necessary at the present level of accu-

Table I. *Wavelengths (in Å) for the $3s^23p\,^2P$–$3s3p^2\,^2S$ and ^2P transitions investigated in this work*

	^2P–^2P		^2P–^2S	
Ion	1/2–1/2	3/2–1/2	1/2–1/2	3/2–1/2
Si II[a]	1193.29	1197.39	1304.37	1309.28
P III[a]	917.12	921.85	998.00	1003.60
S IV[a]	748.40	753.76	809.67	815.95
Cl V[a]	633.19	639.23	681.92	688.93
Ar VI[a]	548.91	555.64	588.92	596.69
K VII[b]	484.26	491.72	517.93	526.45
Ca VIII[c]	432.87	441.09	461.71	471.09
Sc IX[c]	390.89	399.89	416.04	426.26
Ti X[c]	355.82	365.63	378.14	389.24
Fe XIV[c]	257.38	270.51	274.20	289.12
Ni XVI[c]	223.12	237.86	239.51	

[a] Kelly [21].
[b] Ekberg and Svensson [16].
[c] Redfors and Litzén [17].

racy. However, for the heavier ions, measured at Bochum, this effect has been included using an experimentally determined relative efficiency calibration [7].

The low particle density also implies that the beam-foil source is quite weak. This necessitates the use of fast monochromators with rather wide slits (50–100 μm) resulting in line-widths between 0.25 and 1 Å. Hence, line-blending is a potential source of systematic error. This important point will be discussed in detail for the individual measurements described below. However, the beam-foil method also offers two features that help in evaluating this problem. First, blending from lines belonging to a different charge state may be investigated and largely eliminated by changing the beam energy, since this results in different charge-state distributions after the foil. Second, if a potential blend emanates from a level with a shorter lifetime than that of the state of interest, the inherent time-resolution of the beam-foil technique may be utilized by recording the spectra at a distance downstream of the foil (so-called delayed spectra) where the perturbing influence of the blend should be strongly reduced. Both these methods have been used in the present work.

2.2. *Si II and P III*

The measurements in Si II and P III have been performed using the 330 kV accelerator at the University of Toledo [8]. The light emitted after the 2 μg/cm^2 carbon foils was dispersed with a 1 m Acton Research normal-incidence monochromator. The measurements were normalized against beam intensity fluctuations by monitoring the total light emitted immediately behind the foil using a fiber optic light-guide and a photomultiplier tube. For both Si and P, spectra were recorded at beam energies in the range 100 to 250 keV. At these low energies, multiple scattering processes in the foil cause a substantial beam-divergence after the foil, which leads to a noticeable Doppler broadening of the spectral lines. Thus, for the ^{2}P–^{2}S lines in Si II at 1304 and 1309 Å, where a 1200 lines/mm grating was used in conjunction with a Hamamatsu R943-02 photomultiplier, a line-width (FWHM) of 0.8 Å was observed. All other lines were measured with a 2400 lines/mm grating, and a channeltron detector, which resulted in line-widths of around 0.5 Å. For both gratings these widths are about twice the instrumental values.

In Si II both the ^{2}P–^{2}S and ^{2}P–^{2}P multiplets appeared unblended, but because of the Doppler broadening the $^2P_{1/2}$–$^2S_{1/2}$ line at 1304.37 Å is affected by the intense $3s3p\,^3P_2$–$3p^2\,^3P_1$ transition in Si III at 1303.32 Å. However, since the line-separation is 30% larger than the line-widths the overlapping influence of the Si III line can accurately be accounted for by fitting a sum of two Gaussian-shaped components. A total of 19 spectral scans over the ^{2}P–^{2}S lines were made, including 6 measurements at positions downstream of the foil corresponding to a delay-time of 1 or 2 ns. The intensity ratios obtained showed no systematic variations with the different energies (130 and 220 keV) or delay-times used. This supports the assumption that the lines are indeed unblended. The weighted average of the 19 observations is 1.52 ± 0.10 and is included in Table II as our final result. For the ^{2}P–^{2}P transitions, 17 measurements were made, and also in this case consistent intensity ratios were obtained at three different energies (130, 170 and 220 keV) with an average value of 0.54 ± 0.14. The larger relative uncertainty in this case is due to the low intensity observed for these lines, caused by the low efficiency of the channeltron detector in this wavelength range. Because of the poor statistics, measurements with different delay-times were not performed.

Table II. *Experimental and theoretical intensity ratios I (3/2–1/2)/I(1/2–1/2) for the $3s^23p\,^2P_J$–$3s3p^2\,^2S_{1/2}$ and ^2P_J–$^2P_{1/2}$ resonance transitions in the Al-sequence*

	^2P_J–$^2S_{1/2}$		^2P_J–$^2P_{1/2}$	
Spectrum	Experiment	Theory[d]	Experiment	Theory[d]
Si II	1.7[a]	1.67	0.83[a]	0.524
	1.52 ± 0.10[b]		0.54 ± 0.14[b]	
P III	1.40 ± 0.08[b]	1.54	0.60 ± 0.10[b]	0.539
S IV	1.12 ± 0.1[b]	1.38	0.52 ± 0.02[c]	0.559
Cl V	0.87 ± 0.13[c]	1.21	0.58 ± 0.02[c]	0.586
Ar VI	0.75 ± 0.05[c]	1.03	0.61 ± 0.03[c]	0.619
K VII	0.75 ± 0.10[b]	0.856	—	0.662
Ca VIII	—	0.686	—	0.717
Sc IX	0.46 ± 0.04[b]	0.529	—	0.786
Ti X	0.43 ± 0.08[c]	0.391	0.75 ± 0.15[c]	0.874
Fe XIV	0.060 ± 0.01[a]	0.0664	1.2 ± 0.4[a]	1.53
	0.083 ± 0.03[a]			
	0.067 ± 0.02[b]			
Ni XVI	—	0.0150	1.6 ± 0.4[b]	2.14

[a] Solar observations, analysed for optical thickness by Kastner [5].
[b] This work.
[c] Engström *et al.* [1].
[d] Huang [3] (MCDF) and Farrag *et al.* [4] (RELAC).

In P III the $3s^23p\,^2P_{1/2,\,3/2}$–$3s3p^2\,^2S_{1/2}$ transitions are found at 998.0 and 1003.6 Å, respectively, whereas the corresponding transitions from $^2P_{1/2}$ occur at 917.1 and 921.8 Å [9]. The only known blend in any of these lines is the P V $3d\,^2D_{5/2}$–$4p\,^2P_{3/2}$ transition at 997.6 Å [10]. In order to minimize the perturbing influence of this blend the relative intensities in P III were measured at beam energies of 120, 150 and 250 keV, whereas the optimum energy for the production of two-times ionized Phosphorus is around 400 keV. At these low energies less than one percent of the beam after the foil is predicted to be in charge state +4. Despite this low charge state abundance the blend cannot be ignored in an accurate intensity measurement, since even the weaker fine-structure component, $3d\,^2D_{3/2}$–$4p\,^2P_{1/2}$, at 1000.4 Å is observable in the spectra, see Fig. 1. Furthermore, the lifetime of the $4p\,^2P$ levels in P V is 0.4 ns [11] which is almost identical to the 0.48 ns predicted by Huang [3] for $3s3p^2\,^2S$ in P III. Hence, measurements with different delay-times are not an effective tool in this case, and the blend must be deconvoluted from the observed spectra. For this purpose we performed constrained fits of four Gaussian-shaped lines to the observed ^{2}P–^{2}S and ^{2}D–^{2}P peaks. In this process the line separations were fixed to their accurately known values [9, 10], and the intensity ratio of the two P V lines was held constant at the *LS*-coupling value of 9/5. This technique thus takes into account the small but non-negligible wavelength separation between the two blending lines. In all, 18 successful scans over the ^2P_J–$^2S_{1/2}$ lines were analyzed in this way giving an average intensity ratio of 1.40 ± 0.08. Without the blend correction an average of 1.23 was obtained. The ^2P_J–$^2P_{1/2}$ intensity ratio was measured in 20 spectral scans and showed no significant variation with respect to the three energies or to the different delay-times

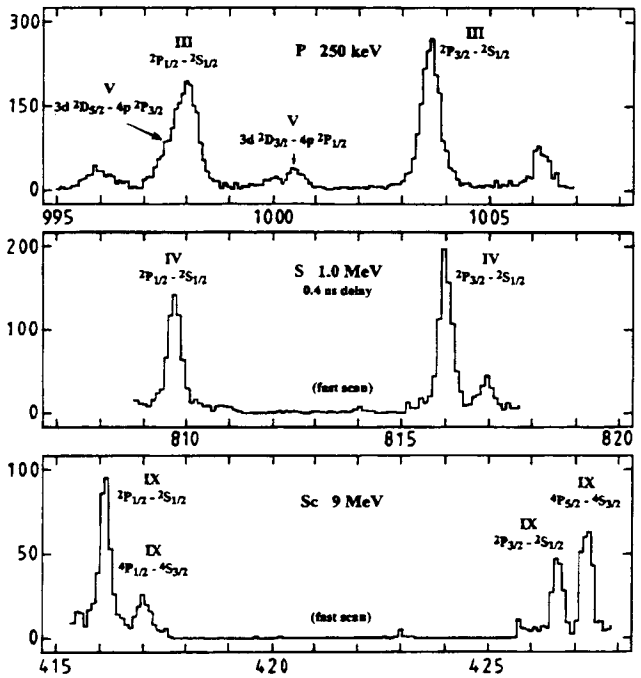

Fig. 1. Beam-foil spectra (intensity in counts *vs.* wavelength in Å) showing the $3s^23p\ ^2P$–$3s3p^2\ ^2S$ transitions in P III, S IV and Sc IX. The P spectrum also contains the $3d\ ^2D$–$4p\ ^2P$ transitions in P V, and in Sc two of the $3s3p^2\ ^4P$–$3p^3\ ^4S$ lines from Sc IX are also included. Note that in S and Sc the interval between the ^2P–^2S peaks has been recorded with very low normalization.

used. Our final results are given in Table II, and represents the weighted average of the individual results.

2.3. *S IV*

In the previous investigation of S IV [1] the intensity ratios were measured at a beam energy of 1.2 MeV. However, at energies of 5 MeV or higher, where the S IV lines have disappeared, a fairly intense line remained at exactly the same wavelength as the $^2P_{1/2}$–$^2S_{1/2}$ transition, i.e. 809.65 Å. At the time of publication of ref. [1] this potential blend was not identified. However, in a subsequent analysis this line has been identified as the $2p^53s3p\ ^2D_{5/2}$ $2p^53p^2\ ^2D_{5/2}$ transition in core-excited Na-like sulphur [12]. Furthermore, an investigation of the relative excitation functions, i.e. light-yield as a function of beam energy, for a number of singly- and doubly-excited states in S V–S IX [13] have shown that the intensity of this core-excited S VI transition may not be negligible even at 1.2 MeV. Hence a remeasurement of the ^2P–^2S intensity ratio in S IV was undertaken in the present study.

The experiment was performed at the 3 MV Pelletron tandem accelerator at the University of Lund and included three main modifications compared to the previous measurement. First the beam energy was lowered to 1.0 MeV (which represents a low-energy record for the machine) to further suppress the S VI line. Secondly, since the blending transition is expected to have a decay time of 0.18 ns with very little cascade feeding [14], compared to 0.30 ns for the $^2S_{1/2}$ level in S IV [15] we recorded spectra with delay times of 0.0, 0.1, 0.2, 0.4 and 0.5 ns. To compensate for beam-fluctuations during the wavelength scans the experimental set-up was modified to allow a photomultiplier to register the total light yield immediately behind the foil, in addition to the normal charge normalization from a Faraday cup. Light normalization was implemented since we found a small but systematic increase in the data collection times, for a fixed amount of charge, as a function of foil exposure time. This observation is interpreted as an increased beam scatter due to foil thickening. Thus, at this low energy an increasing fraction of the beam miss the 1 cm diameter Faraday cup placed 18 cm away from the foil. To test the different normalizations we measured the peak intensities of a number of S IV, S V and S VI lines as a function of foil exposure time. With light normalization the intensities of all the lines remained constant, as expected, whereas charge normalization resulted in a small non-linear increase in the signal after about half the foil lifetime. To further compensate for this effect the ^2P–^2S lines were measured using alternating scan directions.

A total of 17 scans have been measured and the intensity ratio at the foil (zero delay time) is slightly larger (0.9 compared to 0.78) than in Ref. [1], presumably due to the combination of a lower energy and the light normalization. However, at a delay-time of 0.2 ns the ratio has increased to about 1.1. This value then remains constant in the spectra recorded with even larger delays (Fig. 1). Thus, our new result of for S IV is 1.12 ± 0.1, which is clearly in better accord with the isoelectronic trend established in this work.

2.4. *K VII, Sc IX, Fe XIV and Ni XVI*

These measurements have been made at the Dynamitron tandem accelerator at the University of Bochum, using a 2.2 m grazing-incidence monochromator equipped with a 600 lines/mm grating. As mentioned above, the intensity ratios measured at Bochum do include a small correction for the decreasing efficiency of the grazing-incidence instrument with increasing wavelength in the present spectral region [7]. Typical corrections are between 2 and 4%. Further details of the experimental set-up can be found in Ref. [2], which describes similar relative intensity measurements in the B-sequence. Figure 2 shows the isoelectronic evolution of the transition energies for the $3s^23p\ ^2P$–$3s3p^2\ ^2S$ and $3s3p^2\ ^4P$–$3p^3\ ^4S$ multiplets along the Al-sequence. Within the range of ions studied in Bochum two crossings occur in Fig. 2. Thus, in K VII the $^2P_{1/2}$–$^2S_{1/2}$

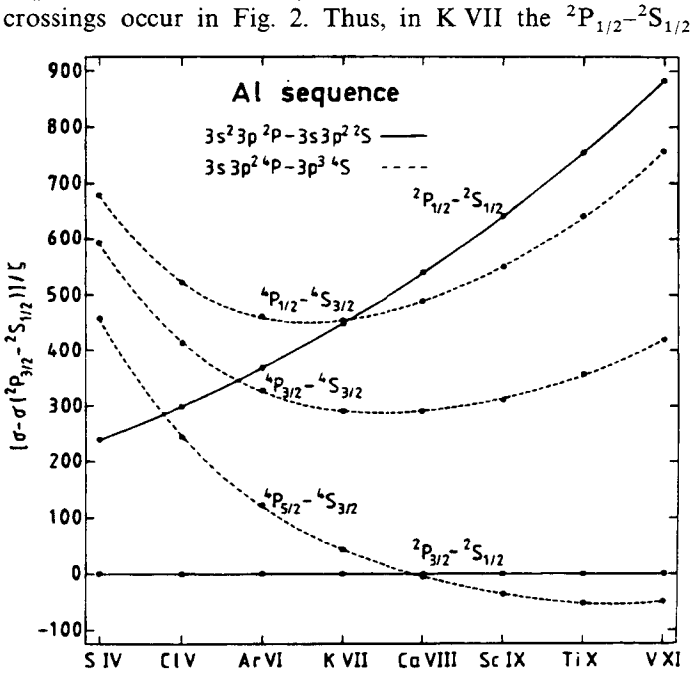

Fig. 2. Isoelectronic plot of the wavenumbers (σ) for the $3s^23p\ ^2P$–$3s3p^2\ ^2S$ and $3s3p^2\ ^4P$–$3p3\ ^4S$ transitions, scaled by the effective nuclear charge (ζ).

transition is blended by the $^4P_{1/2}$–$^4S_{3/2}$ line ($\Delta\lambda = 0.13$ Å), and in Ca VIII the $^2P_{3/2}$–$^2S_{1/2}$ and $^4P_{5/2}$–$^4S_{3/2}$ lines coincide within 0.1 Å [16, 17]. In K VII this blend is corrected for, but Ca VIII, where the blending line is the most intense of the quartet transitions, was not investigated.

In K VII spectral scans were recorded at beam energies of 5 and 7 MeV, covering the wavelength interval 516–527 Å which, in addition to the ^2P–^2S transitions, also contains the two stronger, well resolved components of the ^4P–^4S multiplet. To correct for the $^4P_{1/2}$–$^4S_{3/2}$ blend we used the same technique of constrained Gaussian fits as in P III, discussed above. Thus, all line separations were fixed to the accurate values given in Ref. [16]. Furthermore, the relative intensities of the ^4P–^4S lines were also fixed to the values of 2.88, 1.97 and 1 obtained in a theoretical calculation using the Cowan code [18]. This calculation was performed in a single-configuration mode only, but we note that the results are very close to the *LS* values 3, 2 and 1. In the spectra recorded at the foil (zero delay time) the blend correction amounts to typically 25%. However, the theoretical calculation also shows that the lifetime of the ^4S level is only 0.063 ns compared to the value of 0.17 ns for $^2S_{1/2}$ according to Huang [3]. Hence by again recording delayed spectra the perturbing influence of the blend can be significantly reduced. At a delay time of 50 ps the correction has been reduced to about 11% and at 100 ps delay it is about 8%. The results obtained after the correction at the three delay positions are quite consistent. The final result given in Table II is the average of 5 independent measurements, and the uncertainty quoted includes the estimated statistical error due to the blend correction.

In Sc there are no known lines that should interfere with the measurements. This conclusion is supported by the observed spectrum and the measured line-widths, neither of which indicate the presence of any blends (Fig. 1). The results obtained at 9 and 11 MeV beam energies are also in perfect agreement and our final value given in Table II is the weighted average of 7 independent scans. Because of time limitations the ^2P–^2P intensities in K VII and Sc IX were not measured.

For Fe and Ni we have analyzed spectra recorded previously for other purposes at energies of 20 and 28 MeV, respectively. This material has also been complemented by new measurements in Ni at 36 MeV. Because of the cancellation effects in the $^2P_{3/2}$–$^2S_{1/2}$ transition probability this line becomes progressively weaker in the higher members of the isoelectronic sequence. Thus, while it could be observed in Fe it was completely lost in the background noise in Ni. This trend is consistent with the results of Redfors and Litzén [17] who, using the laser-produced plasma technique, observed the $^2P_{3/2}$–$^2S_{1/2}$ line in all ions between Ca and Fe but not in Co or Ni. In Fe XIV we obtained the intensity ratio of 0.067 ± 0.02. In this case the uncertainty arising from the background correction for the weak $^2P_{3/2}$–$^2S_{1/2}$ line is a substantial factor in the total uncertainty. The quoted error estimate has also been increased from the statistical value of 0.014 to take into account that only one measurement has been made.

In Fe XIV the ^2P–^2P intensity ratio could not be measured because of severe blending by unknown lines in both the 1/2–1/2 and 3/2–1/2 channels. In Ni XVI, on the other hand, both lines appear unblended but the $^2P_{3/2}$–$^2P_{1/2}$ transition at 237.86 Å is affected by the less intense $3s^23d\ ^2D_{5/2}$–$3s3p(^1P)3d\ ^2D_{5/2}$ transition in the same ion at 237.47 Å [17]. In the spectra recorded with 30 or 40 μm slits the observed line widths are slightly smaller than the separation of the two lines and hence quite accurate $^2P_{3/2}$–$^2P_{1/2}$ intensities should be obtained from a fit of two Gaussian shaped components. As an average of 6 measurements we obtain the intensity ratio of 1.6 ± 0.4.

3. Discussion

Table II summarizes the intensity ratios obtained by theory [3, 4], and by solar [5] and laboratory observations in the spectra between Si II nd Ni XVI. This material is also presented in Fig. 3. In Si II and Fe XIV we may compare the two sets of experimental data. The most striking observation is the large deviation of the ^2P–^2P ratio in Si II obtained from the solar analysis with both the laboratory and the theoretical results. However, this discrepancy is most likely due to non-negligible optical thickness in the solar observations, as can be inferred from the analysis by Kastner presented graphically in Fig. 2 of Ref. [5]. For the ^2P–^2S ratio in Si II, on the other hand, the same figure shows that the value of 1.7 obtained should correspond to an optically thin situation, and hence be directly comparable to the beam-foil result. Unfortunately no error estimate is given for the solar data, so the discrepancy between the two results may or may not be significant. In any case we note that the beam-foil value seems to be more consistent with the isoelectronic trend established in this work (Fig. 3). In the case of Fe XIV two results from active regions in the sun are available [5, 19, 20]. For the ^2P–^2S ratio Table II shows that there is perfect agreement between the solar and laboratory results. Hence the value obtained for the ^2P–^2P lines (which could not be measured in this work because of severe blending) from the astronomical observation [19] should most likely also pertain to optically thin conditions, and be directly comparable with the theoretical predictions.

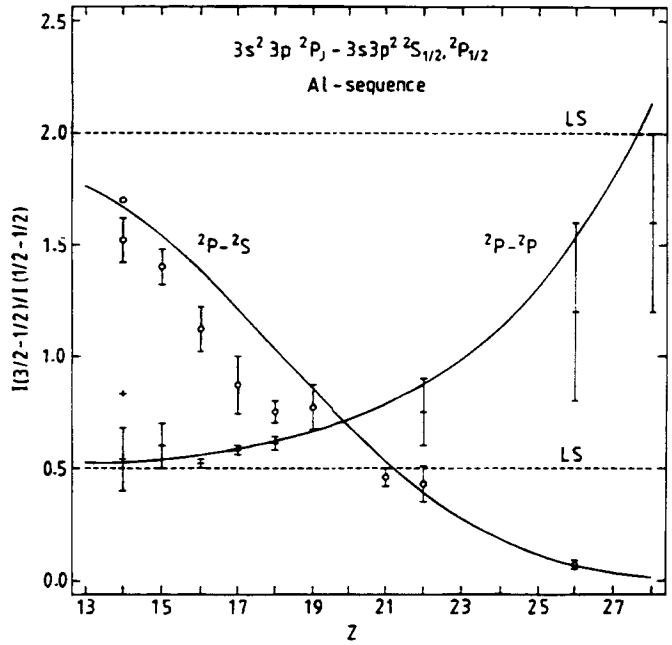

Fig. 3. Experimental intensity ratios for the $3s^23p\ ^2P_J$–$3s3p^2\ ^2S_{1/2}$ (circles) and $^2P_{1/2}$ (+) transitions in the Al I isoelectronic sequence. The smooth curves represent the theoretical predictions [3, 4]. See footnote to Table II for references to the experimental data.

Table II also contains the theoretical results from two relativistic studies of the low-lying levels in the Al-sequence. Of these, Huang [3] uses the MCDF technique with the Breit and Lamb shift contributions to the energies included perturbatively, whereas Farrag *et al.* [4] ignore the higher-order effects in their treatment using the relativistic parametric potential (RELAC) method. Both investigations include the complete $n = 3$ complex to capture the most important correlation effects. The relative intensities, i.e. transition probabilities, obtained in the two theoretical investigations agree to at least two significant digits and are quoted as a single number for each ion in Table II. Both studies give transition energies that are slightly larger than experiment (typically by 2%), but since the different fine-structure components deviate in the same direction the intensity ratios are only marginally affected (<1%) by a scaling with the experimental wavelengths. Furthermore, the important energy separation between the interacting $3s3p^2\ ^2S_{1/2}$ and $^2P_{1/2}$ levels is predicted to better than 2%, typically, in all ions between Si and Ni.

Nevertheless, despite these quality indicators for the theoretical predictions, the results in Table II and Fig. 3 clearly show a systematic discrepancy between theory and experiment concerning the ^2P_J–$^2S_{1/2}$ intensity ratio in the beginning of the sequence. Thus, the present extended experimental investigation confirms the trend observed in Ref. [1]. For the ^2P_J–$^2P_{1/2}$ ratio, on the other hand, the new data for Fe XIV and Ni XVI, together with the previous result in Ti X, seem to indicate a new trend where theory and experiment may diverge for the more highly ionized members of the sequence.

At first sight the combined picture shown in Fig. 3 may be somewhat surprising: Concerning the intensities from the $^2S_{1/2}$ level, theory and experiment disagree in the beginning of the sequence but converge for the higher members, whereas the opposite trend seems to hold in the $^2P_{1/2}$ case. However, one must bear in mind that the experimental intensity ratios test the quality of the theoretical results with quite different sensitivities along the sequence. This important point may perhaps be most clearly seen in a straightforward single-configuration model, which only takes into account the mixing of the three $J = 1/2$ levels of the $3s3p^2$ configuration (^2S, ^2P and ^4P). Within this approximation, Ref. [1] derived simple analytical expressions giving the ratio of the line strengths $R = S(3/2\text{–}1/2)/S(1/2\text{–}1/2)$, i.e. the intensity ratio except for a wavelength dependent factor, from $3s3p^2\ ^2S_{1/2}$ and $^2P_{1/2}$ to the two ground state levels as a function of the ratio (r) of the mixing coefficients of the two doublet levels.

$$R = \begin{cases} \frac{1}{2}\left(1 - \frac{3}{\sqrt{6}\cdot|r|+1}\right)^2 \\ \qquad r = a_2/a_1,\ ^2S = a_1|^2S\rangle + a_2|^2P\rangle + a_3|^4P\rangle, \\ 2\left(1 - \frac{3}{2-\sqrt{2/3}\cdot|r'|}\right)^2 \\ \qquad r' = a'_1/a'_2,\ ^2P = a'_1|^2S\rangle + a'_2|^2P\rangle + a'_3|^4P\rangle. \end{cases}$$

These functions are illustrated for $0 \leqslant |r| \leqslant 1$ in Fig. 2 of Ref. [1].

Numerical values for the mixing coefficients have been obtained from a single-configuration calculation using the Cowan code [18]. The results for a_1 and a_2 are shown in Fig. 4, and to a good approximation $a'_1 = -a_2$ and $a'_2 = a_1$. In Fig. 5 we show the derivative of R with respect to r. The approximate positions on these curves for the different ions from Si to Ni are also indicated using the calculated mixing coefficients (Fig. 4). Comparing Figs 3 and 5 we note that for the intensity ratio from ^2S the discrepancy between theory and experiment occurs in the region of the sequence where the theoretical results are most sensitive to small changes in the composition of the wavefunctions. For the higher members of the sequence the demands on theory are much less severe, and in this range there is good agreement with the experimental results. For the intensities of the tran-

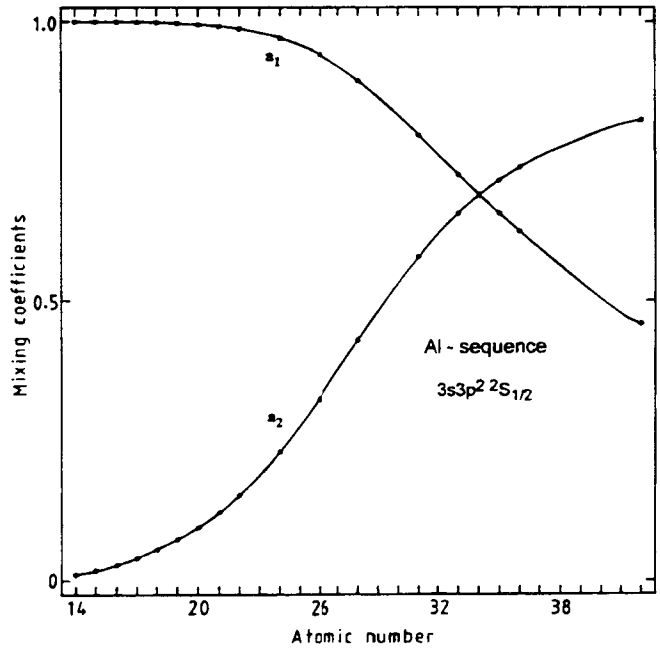

Fig. 4. Isoelectronic evolution of the composition of the state labled $3s3p^2\ ^2S_{1/2}$ in the beginning of the sequence. The results are obtained in a single configuration approximation, i.e. $^2S = a_1|^2S\rangle + a_2|^2P\rangle + a_3|^4P\rangle$. The crossing occurs around Se ($Z = 34$).

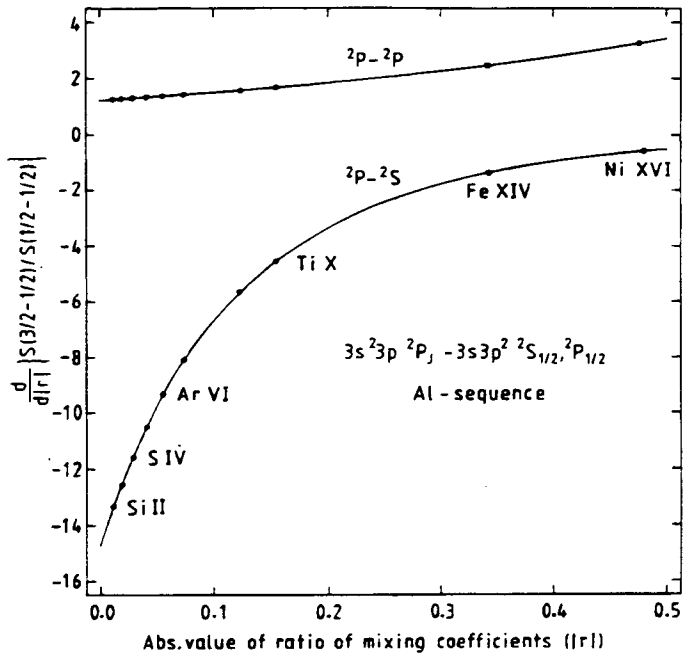

Fig. 5. The derivative of the ratio of the line strengths $S(3/2\text{–}1/2)/S(1/2\text{–}1/2)$ with respect to the absolute value of the ratio (r) of the mixing coefficients between the $3s3p^2\ ^2S_{1/2}$ and $^2P_{1/2}$ levels. These results are obtained from analytical expressions derived in [1], within a single-configuration approximation.

sitions from the $^2P_{1/2}$ level, Fig. 5 shows the opposite isoelectronic trend, although with much less drastic changes. This may explain why theory and experiment agree in the beginning of the sequence, while they seem to diverge for higher ionization stages.

Finally we should also remark that for ions beyond Ni the derivative of the ^2P intensities with respect to the mixing coefficients increases dramatically, and hence experimental studies of the ^2P intensity ratio in this region would be highly desirable as further sensitive tests of the theoretical predictions.

Acknowledgements

This work has been supported by the Swedish Natural Science Research Council (NFR), by Svenska Institutet, and by the U.S. Department of Energy, Office of Basic Energy Sciences, Division of Chemical Sciences under grant number DE-FG05-88ER13958.

References

1. Engström, L., Reistad, N., Jupén, C. and Westerlind, M., Physica Scripta **39**, 66 (1989).
2. Doerfert, J. and Träbert, E., Physica Scripta **47**, 524 (1993).
3. Huang, K.-N., At. Data Nucl. Data Tables **34**, 1 (1986).
4. Farrag, A., Luc-Koenig, E. and Sinzelle, J., At. Data Nucl. Data Tables **27**, 539 (1982).
5. Kastner, S. O., Physica Scripta **50**, 481 (1994).
6. Nicolas, K. R. *et al.*, Solar. Phys. **55**, 305 (1977).
7. Träbert, E., Physica Scripta **T8**, 112 (1984).
8. Haar, R. R. *et al.*, Nucl. Instr. Meth. Phys. Res. **B79**, 746 (1993).
9. Magnusson, C. E. and Zetterberg, P. O., Physica Scripta **15**, 237 (1977).
10. Magnusson, C. E. and Zetterberg, P. O., Physica Scripta **10**, 177 (1974).
11. Lindgård, A. and Nielsen, S. E., At. Data Nucl. Data Tables **19**, 533 (1977).
12. Jupén, C., Engström, L., Hutton, R., Reistad, R. and Westerlind, M., Physica Scripta **42**, 44 (1990).
13. Mönke, D. *et al.*, Phys. Rev. **A49**, 2567 (1994).
14. Bengtsson, P., Westerlind, M., Engström, L. and Jupén, C., Physica Scripta **49**, 303 (1994).
15. Reistad, R. and Engström, L., Phys. Rev. **A39**, 4818 (1989).
16. Ekberg, J. O. and Svensson, L. Å., Physica Scripta **2**, 283 (1970).
17. Redfors, A. and Litzén, U., J. Opt. Soc. Am. **B6**, 1447 (1989).
18. Cowan, R. D., "The Theory of Atomic Structure and Spectra" (University of California Press, Berkeley 1981).
19. Dere, K. P., Solar Phys. **77**, 77 (1982).
20. Malinovsky, M. and Heroux, L., Astrophys. J. 181, 1009 (1973).
21. Kelly, R. L., J. Phys. Chem. Ref. Data **16**, Suppl. 1 (1987).